

# A novel tribasic Golgi export signal directs cargo protein interaction with activated Rab11 and AP-1–dependent Golgi–plasma membrane trafficking

Hirendrasinh B. Parmar<sup>a</sup> and Roy Duncan<sup>a,b,c,\*</sup>

<sup>a</sup>Department of Microbiology and Immunology, <sup>b</sup>Department of Biochemistry and Molecular Biology, and <sup>c</sup>Department of Pediatrics, Dalhousie University, Halifax, NS B3H 4R2, Canada

**ABSTRACT** The reovirus fusion–associated small transmembrane (FAST) proteins comprise a unique family of viral membrane fusion proteins dedicated to inducing cell–cell fusion. We recently reported that a polybasic motif (PBM) in the cytosolic tail of reptilian reovirus p14 FAST protein functions as a novel tribasic Golgi export signal. Using coimmunoprecipitation and fluorescence resonance energy transfer (FRET) assays, we now show the PBM directs interaction of p14 with GTP-Rab11. Overexpression of dominant-negative Rab11 and RNA interference knockdown of endogenous Rab11 inhibited p14 plasma membrane trafficking and resulted in p14 accumulation in the Golgi complex. This is the first example of Golgi export to the plasma membrane that is dependent on the interaction of membrane protein cargo with activated Rab11. RNA interference and immunofluorescence microscopy further revealed that p14 Golgi export is dependent on AP-1 (but not AP-3 or AP-4) and that Rab11 and AP-1 both colocalize with p14 at the TGN. Together these results imply the PBM mediates interactions of p14 with activated Rab11 at the TGN, resulting in p14 sorting into AP1-coated vesicles for anterograde TGN–plasma membrane transport.

**Monitoring Editor**  
Francis A. Barr  
University of Oxford

Received: Dec 18, 2015  
Revised: Feb 17, 2016  
Accepted: Feb 23, 2016

## INTRODUCTION

Trafficking of integral membrane proteins to their correct final destination in specific membrane compartments is essential for normal cell function. Generally, membrane proteins are cotranslationally inserted into the ER membrane directed by a signal peptide (Zimmermann *et al.*, 2011). These proteins are folded and posttranslationally modified as they traffic from the ER to the Golgi complex and *trans*-Golgi network (TGN) via the anterograde secretory pathway and are then sorted into vesicular carriers for transport to the plasma membrane or other membrane organelles (Stenmark, 2009).

This article was published online ahead of print in MBoC in Press (<http://www.molbiolcell.org/cgi/doi/10.1091/mbc.E15-12-0845>) on March 3, 2016.

\*Address correspondence to: Roy Duncan ([roy.duncan@dal.ca](mailto:roy.duncan@dal.ca)).

Abbreviations used: AP, adaptor protein; FAST, fusion-associated small transmembrane; FRET, fluorescence resonance energy transfer; hpt, hours posttransfection; PBM, polybasic motif; RNAi, RNA interference; TGN, *trans*-Golgi network.

© 2016 Parmar and Duncan. This article is distributed by The American Society for Cell Biology under license from the author(s). Two months after publication it is available to the public under an Attribution–Noncommercial–Share Alike 3.0 Unported Creative Commons License (<http://creativecommons.org/licenses/by-nc-sa/3.0>).

“ASCB®,” “The American Society for Cell Biology®,” and “Molecular Biology of the Cell®” are registered trademarks of The American Society for Cell Biology.

Integral plasma membrane proteins are also retrieved from the plasma membrane by endocytosis and recycled back to the plasma membrane or rerouted to lysosomes or other endocytic compartments (Welz *et al.*, 2014). The two major sorting hubs for anterograde and retrograde trafficking—the TGN exocytic hub and the recycling endocytic hub, respectively—are closely entwined in the perinuclear region of cells (Ang *et al.*, 2004; Lock and Stow, 2005; Cancino *et al.*, 2007; Folsch *et al.*, 2009). Considerable effort has been expended on discerning the determinants of cargo protein sorting and the pathways and mechanisms regulating post-Golgi membrane protein trafficking, but our understanding of these processes is far from complete.

Rabs are the largest subfamily of the Ras superfamily of small GTPases and are master regulators of vesicular trafficking (Stenmark, 2009; Hutagalung and Novick, 2011). Rabs exist in two forms—an activated, GTP-bound form and an inactive, GDP-bound form. Guanine nucleotide exchange factors (GEFs) convert inactive GDP-bound Rabs into the active GTP-bound form, and GTPase-activating proteins enhance the Rab GTPase activity, converting the active Rab back into the inactive GDP-bound state. In their active, GTP-bound form, Rab GTPases stably partition into the cytosolic face of

membranes via prenyl groups covalently attached to C-terminal cysteines. Localization of individual Rab proteins to distinct membrane compartments and distinct domains within a given compartment is under complex regulation by numerous factors, including GDP dissociation inhibitors (GDIs), GDI dissociation factors, and GEFs (Barr, 2013; Pfeffer, 2013). Phosphoinositide lipids also provide localization signals for Rab proteins, typified by the well-characterized interaction of Rab5 with phosphatidylinositol 3-phosphate (PI3P) in early endosomes (Vicinanza *et al.*, 2008; Santiago-Tirado and Bretscher, 2011). Coincidence detection of phosphoinositides, small GTPases, and cargo protein-traffic motifs localize cargo to specific organelle microdomains for assembly into transport vesicles.

Studies over the last few years indicate the involvement of complex cascades of small GTPases that sort cargo into adaptor protein (AP)-coated vesicles or tubules. APs are heterotetrameric complexes comprising two large subunits ( $\gamma$ ,  $\alpha$ ,  $\delta$ ,  $\epsilon$ ,  $\zeta$ , and  $\beta$ 1-5), a medium subunit ( $\mu$ 1-5), and a small subunit ( $\sigma$ 1-5; Hirst *et al.*, 2013). Among the various APs, AP-1, AP-3, and AP-4 complexes form distinct vesicles at the TGN for trafficking to endosomes, lysosomes, or the plasma membrane. AP-2 is involved in vesicle formation at the plasma membrane for endocytosis and trafficking to early endosomes; AP-5 is localized to late endosomes, but its precise function is unclear (Ohno, 2006; Hirst *et al.*, 2013; Popova *et al.*, 2013). Sorting cargo into the correct transport pathway is a key step during vesicle formation. Diverse mechanisms exert an influence on this process, including cargo protein interactions with subunits of adaptor coat complexes and with Arf- and Rab-family GTPases (Giraudo and Maccioni, 2003; Mellman and Nelson, 2008; Donaldson and Jackson, 2011; Aloisi and Bucci, 2013). In the case of post-Golgi biosynthetic transport to the plasma membrane, there are only two well-described linear amino acid sorting motifs: tyrosine-based motifs (e.g., Yxx $\phi$  and NPXY, where x is any residue and  $\phi$  is a bulky hydrophobic residue) and dileucine-based motifs (Hunziker *et al.*, 1991; Hunziker and Fumey, 1994; Nishimura *et al.*, 2002; Rodriguez-Boulant *et al.*, 2005). These motifs generally function via interactions with subunits of AP complexes (Ohno *et al.*, 1995; Honing *et al.*, 1998; Mardones *et al.*, 2013; Jia *et al.*, 2014), and their role is more in sorting than Golgi export, since altering these motifs usually leads to cargo protein mislocalization, not failure to exit the Golgi complex (Brewer and Roth, 1991; Rajasekaran *et al.*, 1994).

Of particular importance to post-Golgi protein trafficking is Rab11. Rab11 is most commonly associated with trafficking through the recycling endosome compartment. Recycling endosomes are broadly distributed throughout the cytoplasm, with a concentration in the perinuclear region (Welz *et al.*, 2014). Perinuclear Rab11-positive recycling endosomes are juxtaposed with the TGN, but at steady state, these two compartments remain largely distinct, with only minimal overlap between the staining patterns of Rab11 and TGN markers (Chen *et al.*, 1998; Lock and Stow, 2005; Cheng *et al.*, 2011; Cheng and Filardo, 2012). Nonetheless, there is extensive transient interaction between the TGN and recycling endosomes during both anterograde and retrograde flow of cargo vesicles between the TGN and plasma membrane. There are three isoforms of Rab11: Rab11A, Rab11B, and Rab11C (also known as Rab25; Kelly *et al.*, 2012; Welz *et al.*, 2014). Rab11A is ubiquitously expressed (Kikuchi *et al.*, 1988; Sakurada *et al.*, 1991), Rab11B is predominantly expressed in the brain, heart, and testes (Lai *et al.*, 1994), and Rab25 is expressed in the kidney, lung, and gastric tract (Goldenring *et al.*, 1993). The few examples of Rab11 interaction with cargo proteins involve recycling to the plasma membrane, not transport through the biosynthetic anterograde pathway (Hamelin *et al.*, 2005; van de Graaf *et al.*, 2006; Wikstrom *et al.*, 2008; Parent *et al.*, 2009).

The reptilian reovirus p14 protein is a member of a unique family of virus-encoded, fusion-associated small transmembrane (FAST) proteins. FAST proteins are the smallest known membrane fusion proteins (95–198 residues) and are encoded by the fusogenic reoviruses, the only known nonenveloped viruses that induce syncytium formation (Boutillier and Duncan, 2011). FAST proteins are not constituents of virus particles, but are instead nonstructural viral proteins that are synthesized inside virus-infected cells, where they traffic through the ER–Golgi pathway to the plasma membrane to induce cell–cell membrane fusion. All FAST proteins are bitopic membrane proteins with a single transmembrane domain separating exceedingly small ectodomains (~19–40 residues) from equivalent-sized or considerably larger cytoplasmic endodomains (~40–140 residues; Ciechonska *et al.*, 2014). The p14 FAST protein is a 125-residue protein with a 36-residue myristoylated N-terminal ectodomain and 68-residue cytoplasmic endodomain (Corcoran and Duncan, 2004). The endodomain contains a membrane-proximal cluster of basic residues called the polybasic motif (PBM). We recently determined that p14 PBM functions as a novel tribasic, autonomous Golgi export signal (Parmar *et al.*, 2014b). In the present study, we exploited the simple domain organization and trafficking determinants of the p14 FAST protein to determine how this novel PBM Golgi export signal influences p14 trafficking from the Golgi complex to the plasma membrane. Results indicate a newly identified role for activated Rab11 interaction with membrane cargo at the TGN required for sorting into AP-1-coated vesicles and anterograde Golgi-to-plasma membrane trafficking.

## RESULTS

### Rab11 is required for p14 trafficking from the Golgi complex to the plasma membrane

Alanine substitution of the six basic residues in the cytoplasmic, membrane-proximal PBM of p14 results in p14 accumulation in the Golgi, identifying this motif as a *cis*-acting Golgi export signal (Parmar *et al.*, 2014b). A yeast two-hybrid screen using the cytoplasmic endodomain of p14 as bait identified Rab11A as a potential p14 interaction partner. To determine whether Rab11 has any involvement in p14 trafficking to the plasma membrane, Rab11A activity was inhibited in p14-expressing HeLa cells by transient coexpression of dominant-negative Rab11A-S25N. Western blotting using anti-Rab11A antibody confirmed overexpression of the Rab11A constructs (Figure 1A). Surface expression of p14 was quantified by flow cytometry using a p14 antiserum specific for the N-terminal p14 ectodomain (anti-p14ecto). To remove complications arising from p14-induced syncytium formation (syncytia are incompatible with flow cytometry), we used a fusion-dead p14-G2A construct (hereafter referred to simply as p14) for all experiments. Previous studies indicate that p14-G2A traffics to the plasma membrane as efficiently as authentic p14 (Parmar *et al.*, 2014a,b). Overexpression of Rab11A-S25N reduced p14 surface expression by ~50%, whereas overexpression of wild-type Rab11A or constitutively active Rab11A-Q70L had no effect on p14 plasma membrane trafficking (Figure 1B).

To confirm the dominant-negative Rab11A results, we knocked down Rab11 in HeLa cells using RNA interference (RNAi) to target Rab11A or Rab11B, either individually or in combination. RNAi-mediated knockdown of Rab11A by ~60–70% (Figure 1C) resulted in a significant reduction in p14 surface expression by ~50–60% in cells transfected with small interfering RNA (siRNA) targeting Rab11A or Rab11B and by ~70% in cells containing both siRNAs (Figure 1D). Efficient trafficking of p14 to the plasma membrane is therefore dependent on Rab11. A primary function of Rab11 is receptor recycling to the plasma membrane after

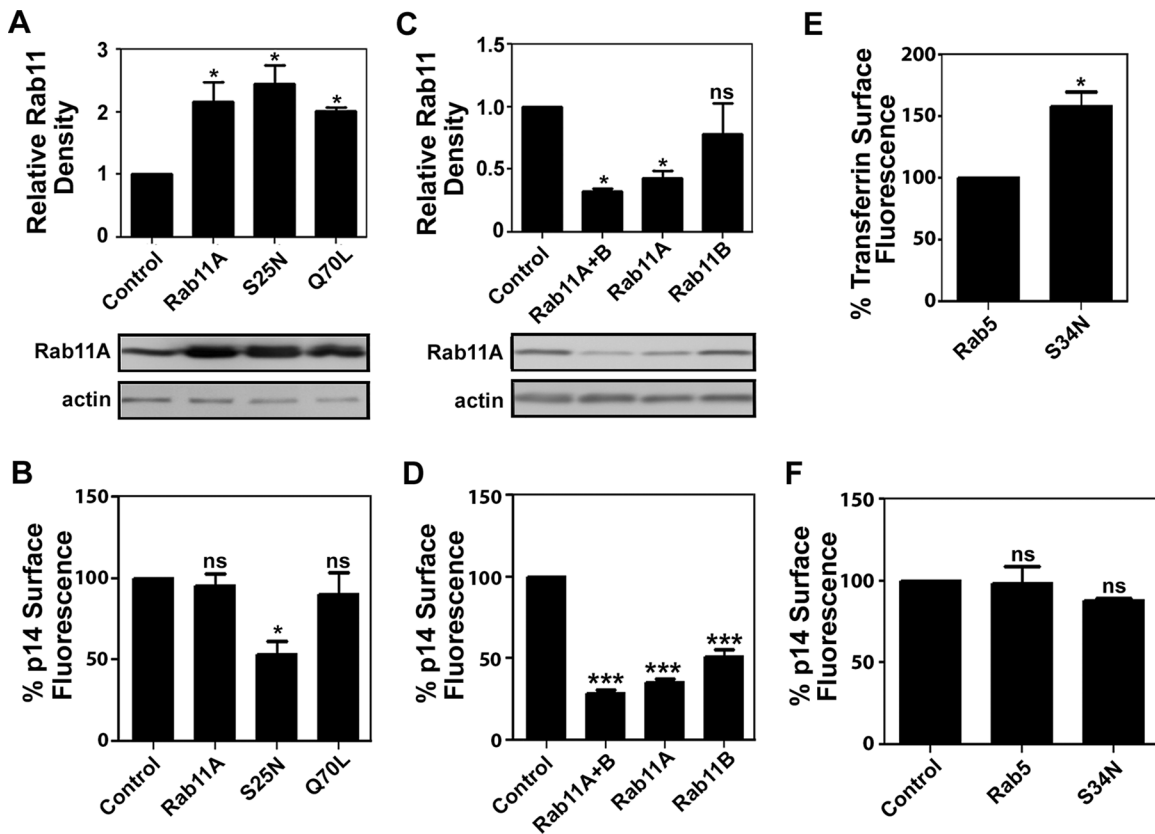


**FIGURE 1:** Rab11 is required for efficient p14 trafficking to the plasma membrane. (A) HeLa cells transfected with Rab11A, Rab11A-S25N (S25N), Rab11A-Q70L (Q70L), or empty vector (control) were harvested at 24 hpt and analyzed by Western blotting with anti-Rab11A antibody. Relative density for Western blots obtained from two independent experiments are shown as mean  $\pm$  SD. (B) HeLa cells cotransfected with p14 and empty vector (Control), Rab11A, Rab11A-S25N (S25N), or Rab11A-Q70L (Q70L) were surface stained at 24 hpt with anti-p14ecto antiserum and Alexa 647 secondary antibody and analyzed by flow cytometry. Percentage cell surface fluorescence relative to control after background subtraction is presented as mean  $\pm$  SEM from three independent experiments performed in triplicate. (C) HeLa cells transfected with siRNA for Rab11A (siRab11A), Rab11B (siRab11B), or both Rab11A and B (siRab11) or control siRNA were harvested at 48 hpt and analyzed by Western blotting with anti-Rab11A antibody. Relative density for Western blots obtained from two independent experiments are shown as mean  $\pm$  SD. (D) HeLa cells were transfected with nontargeting siRNA (Control) or siRNA targeting Rab11A (siRab11A), Rab11B (siRab11B), or both (siRab11A+B), and at 48 hpt were cotransfected with p14. Cells were surface stained for p14 and analyzed by flow cytometry as in B at 24 h after the cotransfection. Percentage cell surface fluorescence relative to control after background subtraction is presented as mean  $\pm$  SEM from three independent experiments performed in triplicate. (E) HeLa cells transfected with Rab5 or Rab5-S34N (S34N) constructs were labeled with Alexa 647–conjugated transferrin at 24 hpt and analyzed by flow cytometry. Percentage transferrin surface fluorescence relative to Rab5-transfected cells is indicated as mean  $\pm$  SEM from three independent experiments performed in triplicate. (F) HeLa cells cotransfected with p14 and Rab5, Rab5-S34N (S34N), or empty vector (Control) were surface stained for p14 and analyzed by flow cytometry as in B. Statistical significance in all graphs was determined by one-way ANOVA and Tukey posttest relative to control, except for E, which used a Student's *t* test relative to Rab5-transfected cells (\* $p < 0.05$ ; \*\*\* $p < 0.001$ ; ns, not significant).

endocytosis (Hamelin *et al.*, 2005; Wikstrom *et al.*, 2008; Stenmark, 2009). To examine whether reduced p14 plasma membrane localization in the presence of Rab11A-S25N reflected inhibited p14 endocytic recycling, we used expression of a Rab5 dominant-negative mutant (Rab5-S34N) to inhibit endocytosis. Rab5-S34N effectively inhibited endocytosis, as shown by increased surface levels of the transferrin receptor (Figure 1E), which is internalized by Rab5-mediated endocytosis (Somsel Rodman and Wandinger-Ness, 2000) but had no effect on p14 surface expression (Figure 1F). Thus Rab11-dependent p14 plasma membrane localization does not reflect the involvement of Rab11 in p14 endocytic recycling.

Immunofluorescence microscopy was used to examine p14 subcellular localization under conditions of limiting Rab11 activity. Confocal microscopy of HeLa cells cotransfected with p14 and nontargeting control siRNA showed punctate p14 staining throughout the cytosol radiating out to the cell periphery, with only minimal colocalization with the PI4KIII $\beta$  Golgi marker (Figure 2). This is the typical staining pattern of p14 undergoing anterograde vesicular transport to the plasma membrane (Parmar *et al.*, 2014b). In contrast, cells expressing the p14PA construct, which contains a polyalanine substitution of the PBM, showed intense colocalization with PI4KIII $\beta$  (Figure 2), evident both visually and by quantifying the Pearson's *r* for 10 cells from each of two independent experiments (Figure 2).

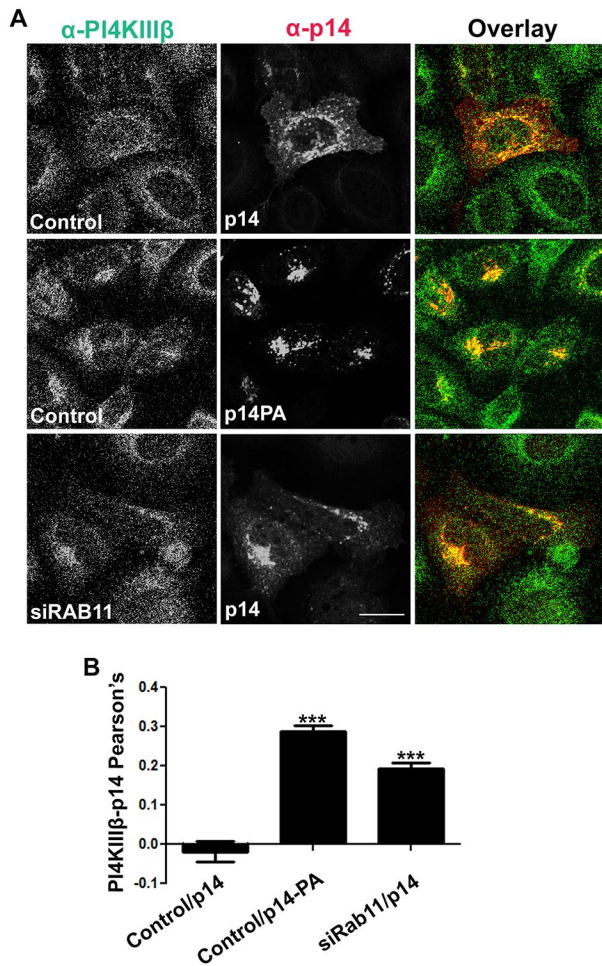


**FIGURE 2:** Rab11 knockdown results in p14 accumulation in the Golgi. (A) HeLa cells were transfected with siRNA targeting Rab11A and B (siRab11) or control siRNA for 48 h and then retransfected with plasmids expressing wild-type p14 (p14) or p14 with an alanine-substituted PBM (p14PA). Cells were fixed, permeabilized, and stained with anti-PI4KIIIβ (green) and anti-p14 (red) antibodies 24 h after plasmid transfection. Right, merged images. Scale bar, 20 μm. (B) Pearson's *r* as mean ± SEM for colocalization between the Golgi marker PI4KIIIβ and p14 for the indicated samples calculated from 20 cells (10 cells from each of two independent experiments). Statistical significance assessed by one-way ANOVA and Tukey posttest is indicated relative to cells cotransfected with control siRNA and p14 (\*\*\*)  $p < 0.001$ .

Inhibiting Rab11A and Rab11B with siRNA resulted in accumulation of p14 in the Golgi complex, similar to what was observed in cells expressing the Golgi export-defective p14PA construct (Parmar *et al.*, 2014b; Figure 2), indicating that Rab11 is required for p14 trafficking from the Golgi complex to the plasma membrane.

### The PBM is required for p14 interaction with activated GTP-Rab11

To interrogate the mechanism by which Rab11 mediates p14 plasma membrane trafficking, we immunoprecipitated cell lysates from HEK cells expressing p14 or p14PA with anti-Rab11A antibody and probed Western blots with anti-p14 antiserum. As shown, p14 coimmunoprecipitated with Rab11A (Figure 3A, lane 2), whereas p14PA was detected at only background levels equivalent to those obtained using a heterologous immunoglobulin G (IgG) isotype anti-

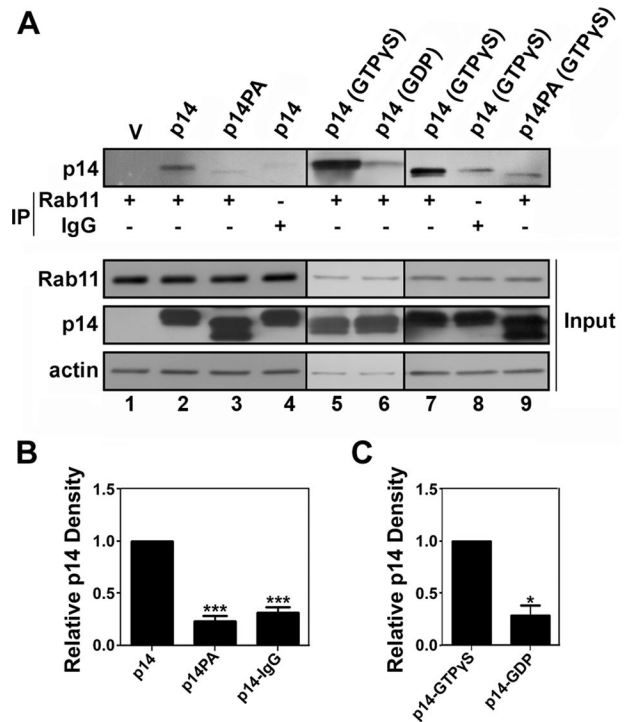


**FIGURE 3:** p14 preferentially interacts with activated Rab11 in a PBM-dependent manner. (A) Lysates of HEK cells transfected with plasmids expressing wild-type p14 (p14) or p14 with an alanine-substituted PBM (p14PA) or empty vector (V) were immunoprecipitated with anti-Rab11 antibody at 24 hpt, either with no treatment or after addition of GTPγS or GDP as indicated. An irrelevant IgG antibody was used as a negative isotype control. Immunoprecipitated samples (top) and lysates before immunoprecipitation (bottom three) were processed by Western blotting using anti-p14, anti-Rab11, and anti-actin antibodies. (B) Quantified Western blots obtained from three independent experiments as described in A are shown as mean ± SEM relative to p14-transfected cells. The p14 and p14PA samples were immunoprecipitated with anti-Rab11 antibody, or the p14 sample was immunoprecipitated using the IgG isotype control (p14-IgG). (C) Quantified Western blots obtained from three independent experiments as described in A, using p14-transfected cell lysates treated with GTPγS or GDP before immunoprecipitation with α-Rab11 antibody. Results are shown as mean ± SEM relative to GTPγS-treated samples. Statistical significance in B and C was determined by one-way ANOVA and Tukey posttest (\* $p < 0.05$ ; \*\*\* $p < 0.001$ ).

body as a negative control for the immunoprecipitations (Figure 3A, lanes 4 and 8). Most notably, when GTPγS (a nonhydrolyzable analogue of GTP) or GDP was added to cell lysates before immunoprecipitation, there was a marked increase in coprecipitation of p14 by anti-Rab11A antibody in lysates enriched for the GTP-bound form of Rab11 (Figure 3A, lane 5 versus lane 6). Even in the presence of GTPγS, p14PA still failed to coprecipitate with anti-Rab11A antibody above the background level observed with the negative isotype control (Figure 3A, lanes 8 and 9). As an aside, two distinct p14 polypeptides were apparent in cell lysates expressing p14PA but not p14 (Figure 3A, input samples, lanes 3 and 9). This doublet was not observed in previous studies with p14PA (Parmar *et al.*, 2014a,b), in which cell lysates were analyzed at 8 h posttransfection (hpt) instead of 24 hpt as in the present experiments. Time-course studies indicated the lower p14PA band accumulates over time (Supplemental Figure S1), most likely due to aberrant accumulation of

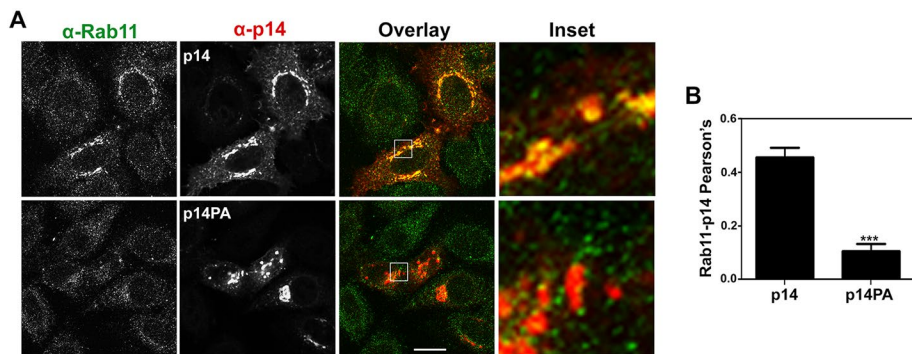


**FIGURE 4:** p14 colocalizes with Rab11 in cells in a PBM-dependent manner. (A) HeLa cells transfected with plasmids expressing wild-type p14 (p14) or p14 with an alanine-substituted PBM (p14PA) were fixed, permeabilized, and stained with anti-Rab11 (green) and anti-p14 (red) antibodies at 24 hpt. An overlay of the two images is shown in color, with the boxed areas shown as enlargements in the right images. Scale bar, 20  $\mu$ m. (B) Pearson's  $r$  as mean  $\pm$  SEM for colocalization between Rab11 and p14 or p14PA calculated from 20 cells (10 cells in each of two independent experiments). Statistical significance is indicated by Student's  $t$  test ( $***p < 0.001$ ).

p14PA in the Golgi complex leading to lysosomal trafficking and degradation of the luminal p14 ectodomain. The coimmunoprecipitation results imply that p14 interacts preferentially with activated Rab11 in a PBM-dependent manner.

The coimmunoprecipitation results were supported by immunofluorescence microscopy using anti-p14 and anti-Rab11 antibodies to stain HeLa cells expressing p14 or p14PA. As previously reported (Parmar *et al.*, 2014b), p14PA fails to traffic to the plasma membrane and accumulates in perinuclear foci that correspond to the Golgi complex and TGN (Figure 4). Visually, there was minimal colocalization of p14PA with Rab11, which was confirmed by a low Pearson's  $r$  (Figure 4). In contrast, p14 staining was broadly distributed in puncta throughout cells, with obvious concentration in the perinuclear region (Figure 4). Furthermore, there was clear evidence of Rab11 redistribution in cells expressing p14, from distributed punctate staining throughout the cytoplasm to concentrated perinuclear staining that extensively colocalized with p14 (Figure 4). Thus both in vitro and in cells (i.e., in cultured cells) results support the conclusion that p14 interacts with Rab11 in a PBM-dependent manner.

#### PBM-dependent interaction of p14 with activated Rab11 in cells

To determine whether the interaction between p14 and Rab11 in cells might be direct, we performed fluorescence resonance energy transfer (FRET) experiments in HeLa cells using fluorescently tagged p14 and Rab11 proteins. FRET analysis identifies protein–protein interactions that occur over distances of  $<5$ – $10$  nm (Sekar and Periasamy, 2003), a spatial separation consistent with direct protein–protein interaction. The p14 and p14PA proteins were C-terminally tagged with enhanced green fluorescent protein (EGFP), and Rab11A and Rab11A-S25N were N-terminally tagged with mCherry. Fluorescently tagged p14 and Rab11 were previously shown to maintain their normal endogenous cellular localization pattern (Rzomp *et al.*, 2003; Corcoran *et al.*, 2011b). Donor and acceptor spectral bleedthrough (SBT) values and normalized FRET (NFRET) intensities were determined using the PixFRET ImageJ plug-in (Feige *et al.*, 2005), as previously reported (Ciechonska *et al.*, 2014; Key and Duncan, 2014). Mean NFRET values (mNFRET) were determined for 10 cells in each of two separate experiments. Cells coexpressing EGFP- and mCherry-tagged p14 were used as a positive control for bimolecular FRET, since previous studies indicated that

p14 forms homomultimers that are detectable in cells by FRET (Corcoran *et al.*, 2011a; Ciechonska *et al.*, 2014; Key and Duncan, 2014). Cells coexpressing free EGFP and mCherry-Rab11, or free mCherry and p14-EGFP, were used as negative FRET controls (Supplemental Figure S2). Based on mNFRET values, cells coexpressing mCherry-Rab11A and p14-EGFP emitted FRET signals equivalent to those obtained from cells coexpressing p14-EGFP and p14-mCherry (Figure 5), indicating that Rab11A and p14 form heteromultimers in cells. Cells coexpressing p14-EGFP and the mCherry-tagged dominant-negative Rab11A-S25N failed to provide FRET signals above background (Figure 5), supporting the coimmunoprecipitation results indicating that the active, GTP-bound form of Rab11 is required for efficient interaction with p14. Cells coexpressing mCherry-Rab11A and

p14PA-EGFP also failed to provide any significant FRET signals (Figure 5), again consistent with the in vitro coimmunoprecipitation results indicating that p14 PBM is required for efficient p14 interaction with Rab11. Together these results imply that p14 directly interacts with Rab11 in a PBM-dependent manner.

#### Anterograde Golgi-plasma membrane transport of p14 is dependent on AP-1-coated vesicles

Trafficking from the TGN is dependent on APs that form vesicle coat complexes during vesicle formation. In particular, AP-1, AP-3, and AP-4 are involved in vesicle transport between the TGN and endosomes, lysosomes, and the plasma membrane (Ohno, 2006; Popova *et al.*, 2013). To examine which APs play a role in Rab11-mediated p14 trafficking to the plasma membrane, we used pooled siRNAs targeting expression of the large  $\gamma$ ,  $\delta$ , or  $\epsilon$  subunits to knock down AP-1, AP-3, or AP-4 complexes, respectively. Western blotting indicated all three siRNAs reduced expression of their respective AP subunit by  $\sim 70$ – $90\%$  (Figure 6B and Supplemental Figure S3). However, only AP-1 knockdown resulted in a significant, 50% decrease in p14 plasma membrane expression as analyzed by flow cytometry (Figure 6A). To confirm that the AP-1 results were due to specific knockdown of AP-1 and not off-target siRNA artifacts, we subsequently cotransfected cells transfected with control or AP-1 siRNA pools with plasmids expressing p14 and AP-1. Overexpression of AP-1 in control siRNA-transfected cells led to a significant increase in p14 trafficking to the plasma membrane, whereas AP-1 overexpression in cells transfected with AP-1 siRNA restored p14 plasma membrane expression to levels not significantly different from those obtained in control siRNA-transfected cells (Figure 6C). Immunofluorescence microscopy also revealed that AP-1 knockdown resulted in p14 redistribution to the Golgi complex, as shown by intense colocalization of p14 with PI4KIII $\beta$  (Figure 7). This p14 staining pattern mimicked that of normal cells expressing the transport-deficient p14PA PBM mutant (Figure 2A). In contrast, there was no marked differences in the p14 staining pattern in cells expressing siRNAs targeting AP-3 or AP-4 (Figure 7) compared with normal cells (Figure 2A), indicating that efficient p14 export from the Golgi complex and trafficking to the plasma membrane is solely reliant on AP-1-coated vesicles.

Because knockdown of either Rab11 or AP-1 resulted in p14 accumulation in the Golgi complex, it seemed likely that Rab11

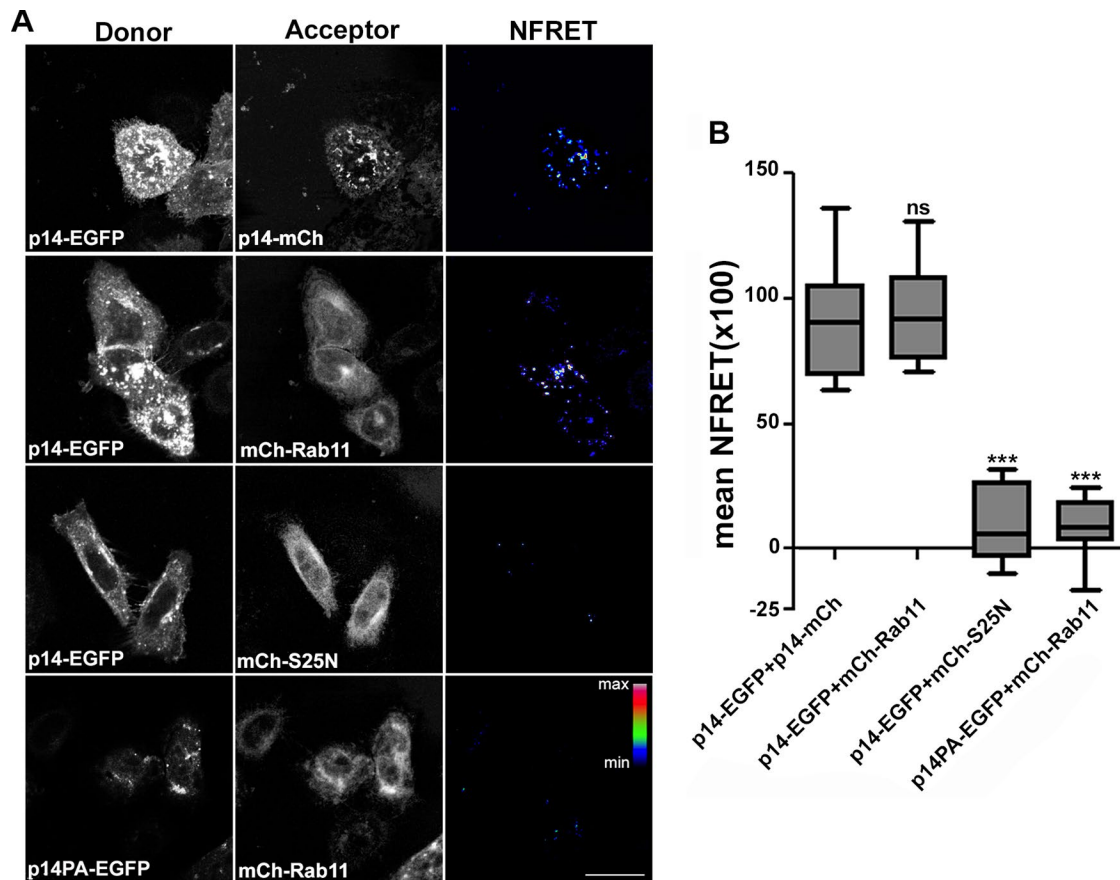


**FIGURE 5:** p14 interacts with Rab11 in cells in a PBM-dependent manner. (A) HeLa cells cotransfected with p14 or p14PA tagged with EGFP and Rab11 or Rab11-S25N (S25N) tagged with mCherry (mCh) were fixed at 24 hpt and imaged for sensitized emission FRET along with donor and acceptor images. Right, calculated normalized FRET (NFRET) images. Cells cotransfected with p14 tagged with EGFP (p14-EGFP) and mCherry (p14-mCh) were used as a positive FRET control for a known multimeric membrane protein. NFRET range is indicated by color gradations. Scale bar, 20  $\mu$ m. (B) Mean NFRET values were calculated for 20 cells (10 cells from each of two independent experiments) for the indicated cotransfected samples. Boxes indicate SDs, horizontal lines indicate means, and whiskers indicate minimum and maximum mean NFRET values. Statistical significance by one-way ANOVA and Tukey posttest relative to the positive control (cells cotransfected with p14-EGFP and p14-mCh; \*\*\* $p < 0.001$ ; ns, not significant).

and AP-1 mediate p14 trafficking from the TGN sorting hub to the plasma membrane. To examine directly whether this might be the case, we triple stained HeLa cells expressing p14 using antibodies against p14, a TGN marker (TGN46), and either Rab11 or AP-1. At steady state, AP-1 extensively colocalizes with the TGN, whereas Rab11 is found predominantly in recycling endosomes (Cheng *et al.*, 2011; Guo *et al.*, 2013). This was the case in mock-transfected HeLa cells (Figure 8B) and cells expressing low or undetectable levels of p14 in p14-transfected cell cultures (Figure 8A), where AP-1 displayed substantial colocalization with TGN46, whereas there was only minimal overlap in Rab11 and TGN46 staining patterns. In p14-transfected cells, p14 was extensively colocalized with TGN-associated AP-1. Most notably, p14 expression led to substantial and significant redistribution of Rab11 to the TGN (Figure 8C), similar to the altered Rab11 staining pattern noted in p14-expressing cells (Figure 4). The redistribution of Rab11 to the TGN and strong colocalization of p14 and TGN46 with both Rab11 and AP-1 suggests p14 recruits Rab11 to the TGN to mediate sorting into AP-1-coated vesicles and Golgi-plasma membrane transport of p14.

## DISCUSSION

Intracellular protein trafficking is a tightly regulated process requiring recognition of *cis*-acting trafficking motifs in cargo proteins or cargo protein receptors by *trans*-acting cellular decoding machinery to direct proteins to their respective subcellular compartments. Although the TGN is considered a central station for sorting and trafficking of proteins transiting through the secretory pathway (Wilson *et al.*, 2011; Bankaitis *et al.*, 2012), the mechanisms governing exit from the Golgi complex to the plasma membrane remain poorly understood. We recently identified a novel *cis*-acting trafficking motif that functions as a tribasic Golgi export signal capable of mediating Golgi export not only of the p14 FAST protein but also of a heterologous Golgi-resident protein (Parmar *et al.*, 2014b). We now show that 1) p14 trafficking from the Golgi complex to the plasma membrane is dependent on Rab11; 2) the PBM is required for preferential interaction of p14 with activated GTP-Rab11, both *in vitro* and *in cells*; 3) AP-1-coated vesicles are specifically involved in p14 plasma membrane trafficking; and 4) p14, Rab11, and AP-1 all colocalize in the TGN. Together our results imply the PBM mediates interactions of p14 with activated Rab11 at the TGN, resulting in

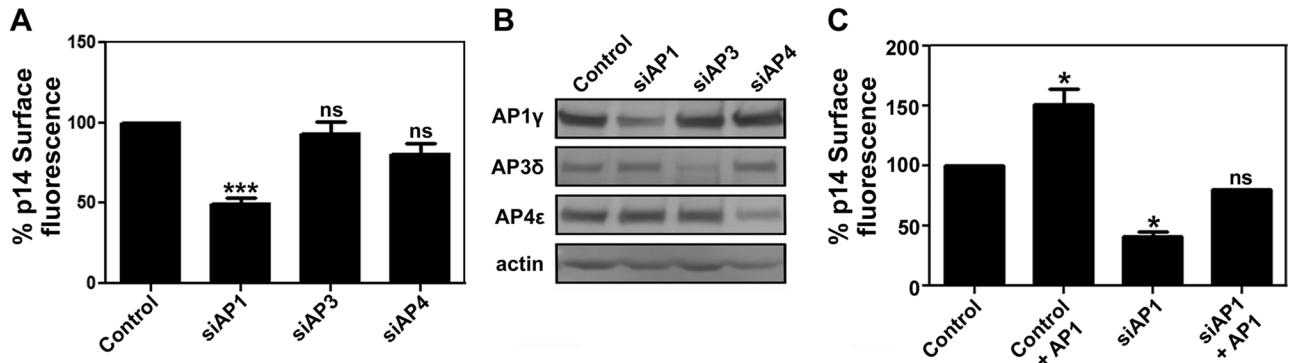


**FIGURE 6:** p14 plasma membrane trafficking is dependent on AP-1. (A) HeLa cells transfected with control siRNA or siRNA targeting AP-1 $\gamma$  (siAP1), AP-3 $\delta$  (siAP3), or AP-4 $\epsilon$  (siAP4) for 48 h were retransfected with p14 for 24 h and then analyzed for p14 cell surface fluorescence by flow cytometry as in Figure 1B. Percentage cell surface fluorescence relative to control siRNA-transfected cells is indicated as mean  $\pm$  SEM from three independent experiments performed in triplicate. (B) Lysates of HeLa cells transfected with the indicated siRNAs were subjected to Western blotting with anti-AP-1 $\gamma$ , anti-AP-3 $\delta$ , anti-AP-4 $\epsilon$ , or anti-actin antibodies at 48 hpt. (C) As in A, except that cells transfected with control or AP-1–targeted siRNAs were subsequently cotransfected with p14 and a plasmid expressing the AP-1  $\gamma$ 1 subunit. Percentage cell surface fluorescence relative to control siRNA–transfected cells is indicated as mean  $\pm$  SEM from two independent experiments performed in triplicate. Statistical significance in A and C by one-way ANOVA and Tukey posttest is indicated relative to control siRNA-transfected cells (\* $p < 0.05$ ; \*\*\* $p < 0.001$ ; ns, not significant).

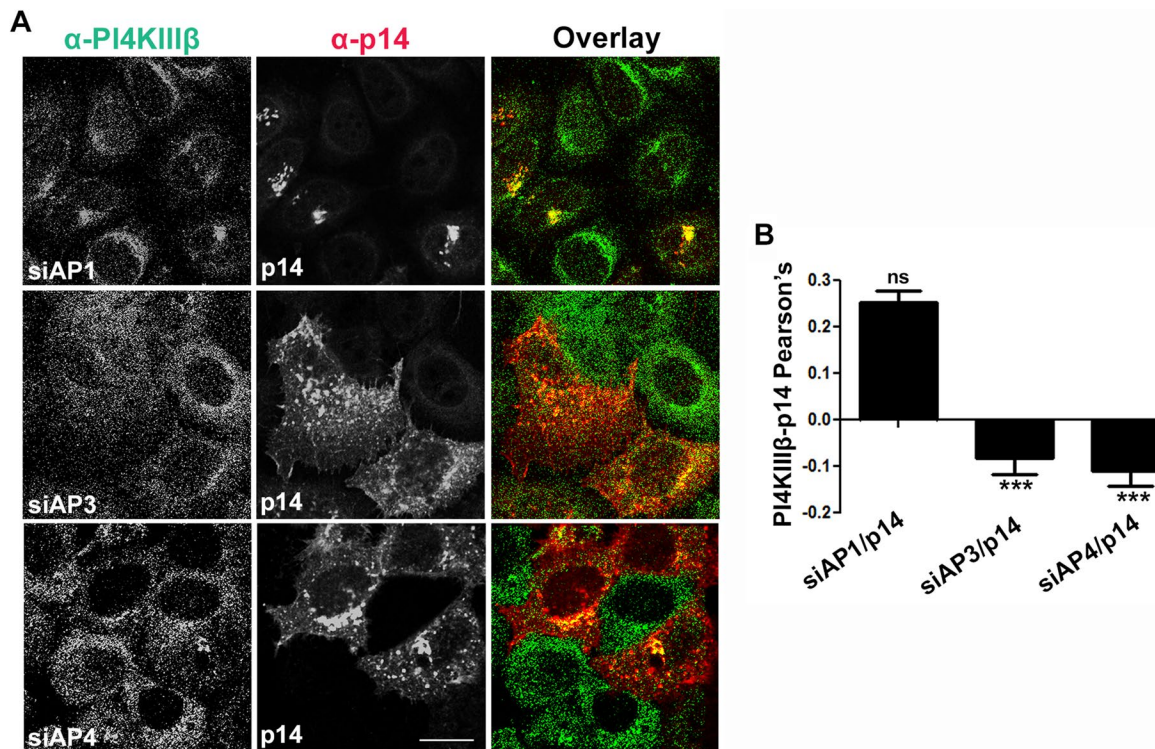


**FIGURE 7:** Knockdown of AP-1 results in p14 accumulation in the Golgi complex. (A) HeLa cells transfected with siRNA targeting AP-1 $\gamma$  (siAP1), AP-3 $\delta$  (siAP3), or AP-4 $\epsilon$  (siAP4) were retransfected at 48 hpt with p14 for 24 h and fixed, permeabilized, and stained with anti-PI4KIII $\beta$  (green) and anti-p14 (red) antibodies. Right, merged images. Scale bar, 20  $\mu$ m. (B) Pearson's  $r$  for colocalization between Golgi marker PI4KIII $\beta$  and p14 is shown as mean  $\pm$  SEM for the indicated samples calculated from 20 cells (10 cells from each of two independent experiments). Statistical significance by one-way ANOVA and Tukey posttest is indicated relative to cells cotransfected with AP-1 $\gamma$  siRNA and p14-G2A (\*\*\* $p < 0.001$ ; ns, not significant).

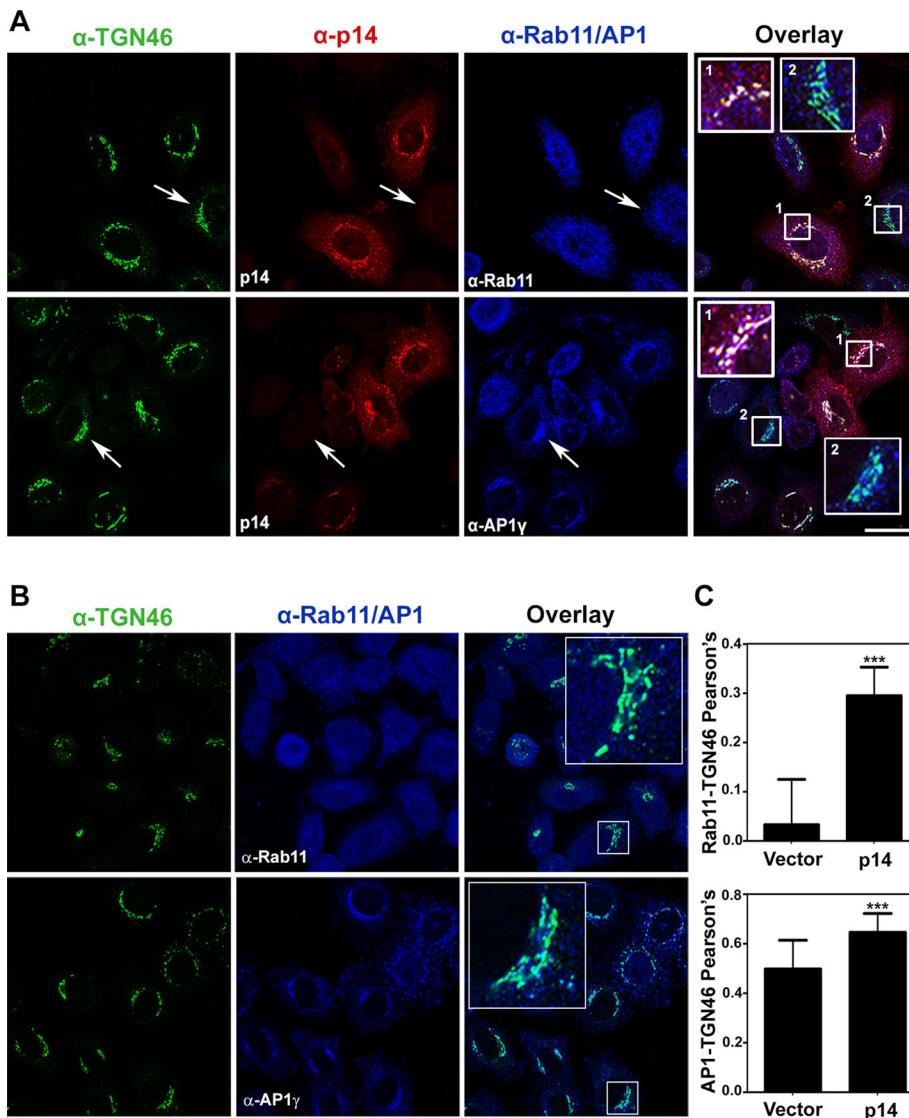


**FIGURE 8:** p14 redistributes Rab11 to the TGN, and p14 colocalizes with Rab11 and AP-1 at the TGN. (A) HeLa cells transfected with p14 were fixed, permeabilized, and stained with anti-TGN46 (green), anti-p14 (red), and anti-Rab11 (blue) or anti-AP1 $\gamma$  (blue) antibodies at 24 hpt. Right, overlay of the three images. Arrows indicate cells expressing low or undetectable levels of p14, and a boxed region of these cells (labeled box 2 in each overlay) is enlarged in the insets. A region from p14-expressing cells (labeled box 1 in each overlay) is enlarged in the corresponding insets. Scale bar, 20  $\mu$ m. (B) Mock-transfected HeLa cells were fixed, permeabilized, and stained with anti-TGN46 (green) and anti-Rab11 (blue) or anti-AP1 $\gamma$  (blue) antibodies at 24 hpt. Right, overlay of the two images. Boxed regions in the overlay are enlarged in the insets. (C) Pearson's *r* for colocalization between TGN46 and Rab11 (top) or AP-1 (bottom) in mock vector-transfected or p14-transfected cells. Results are shown as mean  $\pm$  SEM for 20 cells, and statistical significance was assessed by Student's *t* test (\*\*\*)  $p < 0.001$  relative to vector-transfected cells.

p14 sorting into AP-1-coated vesicles and anterograde transport from the TGN to the plasma membrane (Figure 9).

Several studies document the interaction of cargo proteins with Rab11 but not generally with GTP-Rab11 and not for anterograde transport from the Golgi complex. Instead, the predominant defined role of Rab11 interaction with cargo proteins involves sorting in the endocytic compartment for recycling back to the plasma membrane based on cargo protein interactions with GDP-bound Rab11 (Aloisi and Bucci, 2013). Examples include the TRPV5/6 Ca<sup>2+</sup>-selective members of the transient receptor potential (TRP) channel

superfamily (van de Graaf *et al.*, 2006) and G protein-coupled receptors such as the  $\beta$ 2-adrenergic ( $\beta$ 2AR) and thromboxane A2 receptor  $\beta$ -isoform (TP $\beta$ ) receptors (Hamelin *et al.*, 2005; Parent *et al.*, 2009). Interactions of the human prostacyclin receptor (hIP) with Rab11 is also required for hIP recycling to the plasma membrane, but coimmunoprecipitation indicated no preference for GTP- or GDP-bound Rab11 (Wikstrom *et al.*, 2008). In contrast, coimmunoprecipitation assays (Figure 3) and in cella FRET analysis (Figure 5) indicated a clear preference for p14 interaction with GTP-Rab11. Furthermore, Rab11-S25N localizes to the TGN (Chen *et al.*, 1998), where it could interact with p14 but, based on FRET analysis, does not (Figure 5), consistent with the conclusion that p14 interacts with activated GTP-Rab11.

We are aware of only two examples in which the active form of Rab11A interacts with cargo proteins; the voltage-gated potassium channel Kv1.5 and the CXCR1 and CXCR2 interleukin-8 (IL-8) receptors (McEwen *et al.*, 2007; Takahashi *et al.*, 2007). In both cases, Rab11 mediates cargo protein recycling back to the plasma membrane, and it is not known whether the IL-8 receptors or Kv1.5 directly interact with Rab11. GTP-bound Rab25, an epithelial-specific member of the Rab11 subfamily (also known as Rab11C), has been shown to directly interact with the  $\alpha$ 5 $\beta$ 1 integrin cargo protein (Caswell *et al.*, 2007), but, as with the IL-8 receptors and Kv1.5, this interaction promotes endocytic recycling back to the plasma membrane. In contrast, several lines of evidence indicate that p14 recruits activated Rab11 for exocytic trafficking from the Golgi complex to the plasma membrane: 1) prior results obtained using endocytosis inhibitors (Parmar *et al.*, 2014b) and the present results using Rab5-S34N (Figure 1F) indicate that p14 is not subject to rapid or extensive endocytosis; 2) inhibiting Rab11 activity decreases p14 cell surface expression and leads to extensive p14 accumulation in the Golgi complex (Figure 2); 3) p14 expression results in Rab11 redistribution and colocalization with p14 in the perinuclear region in a PBM-dependent manner (Figure 4); and 4) Rab11 colocalizes with p14 at the TGN (Figure 8). These results, coupled with the coimmunoprecipitation and FRET results, indicate that GTP-Rab11 interacts with the p14 membrane cargo protein to mediate exit from the TGN and biosynthetic Golgi-plasma membrane trafficking. Although cargo protein interactions with numerous different GTP-bound Rabs, including Rabs1, 4, and 21, are known to influence endocytosis, plasma membrane recycling, and lysosome sorting (Pellinen *et al.*, 2006; McEwen *et al.*, 2007; Hammad *et al.*, 2012), this is the first example of cargo protein

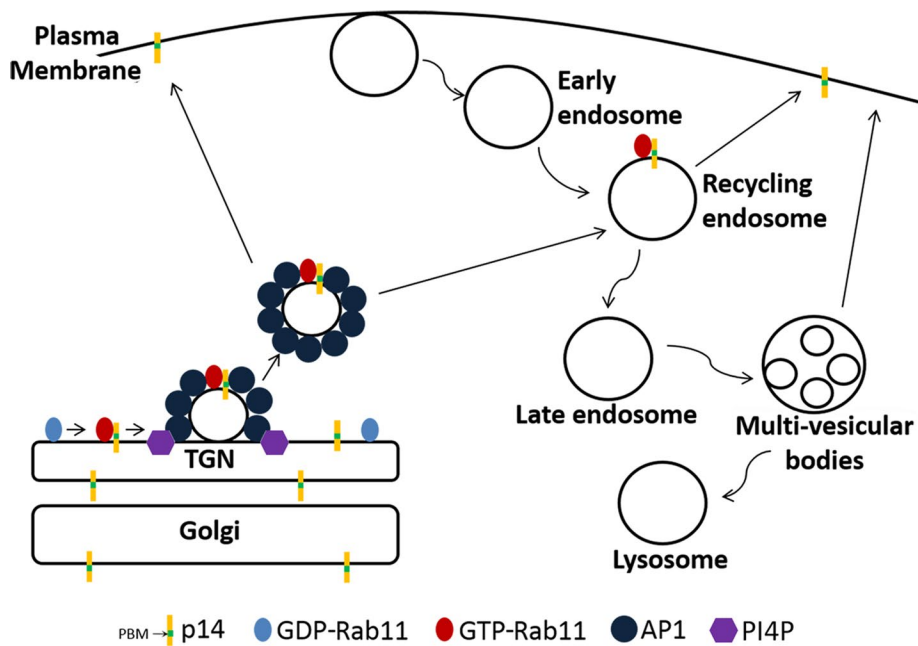


**FIGURE 9:** Model for p14 plasma membrane trafficking from the TGN. The p14 PBM directs interaction with activated GTP-Rab11 bound to the TGN membrane, possibly involving interactions with TGN-localized phosphoinositide lipids such as PI4P. These interactions sort p14 into vesicles being formed by the AP-1 adaptor complex, which then traffic from the TGN to the plasma membrane either directly or via the endosomal recycling pathway.

interaction with activated Rab11 mediating anterograde trafficking from the TGN.

The functionally relevant interaction of p14 with GTP-Rab11 in p14 trafficking suggests that p14 functions as a Rab11 effector. Both AP-1 and Rab11 are involved in bidirectional transport between the TGN exocytic hub and the recycling endocytic hub. AP-1 is known to colocalize extensively with the TGN (Wang *et al.*, 2003); we showed a similar colocalization in mock-transfected cells and colocalization of AP-1 with both p14 and TGN46 in p14-transfected cells (Figure 8). Furthermore, AP-1 knockdown leads to decreased p14 trafficking to the plasma membrane and p14 accumulation in the Golgi complex (Figures 6 and 7), indicating that AP-1 mediates anterograde transport of p14 from the TGN to the plasma membrane. Steady-state Rab11 localization is predominantly in recycling endosomes and to a lesser extent in TGN (Lock and Stow, 2005; Cheng *et al.*, 2011; Cheng and Filardo, 2012). We observed a substantial and significant increase in colocalization of Rab11 and TGN46 in p14-expressing cells (Figure 8), an observation consistent with stabilized membrane partitioning of Rabs after binding to cognate effectors (Pfeffer, 2013). It is not clear whether p14 expression hijacks Rab11 to mediate TGN export, diverting it from its role in the recycling endosome compartment, or whether formation of TGN export vesicles is a normal physiological function of Rab11. The latter possibility is consistent with steady-state colocalization of Rab11 with the TGN, albeit at low levels in most cell types. It is possible that Rab11 normally interacts with the TGN in a transient manner to promote vesicle biogenesis and that this transient interaction becomes more apparent as Rab11 interacts with the excess levels of this viral membrane cargo protein transiting through the TGN. The present results also do not exclude a possible role for recycling endosomes in p14 trafficking. Recycling endosomes are juxtaposed to the TGN, and studies in polarized and nonpolarized cells indicate that vesicles exiting the TGN can rapidly merge with perinuclear Rab11-positive recycling endosomes before trafficking to the plasma membrane

(Futter *et al.*, 1995; Ang *et al.*, 2004; Lock and Stow, 2005; Cancino *et al.*, 2007). A similar transport pathway may apply to Rab11/AP-1/p14 vesicles exiting the TGN.

Interaction of Rabs with various cargo protein-sorting motifs is a feature of Rab-regulated intracellular trafficking (Aloisi and Bucci, 2013), although there is no clearly defined consensus motif for cargo protein-Rab GTPase interactions. Furthermore, the same sorting motif can mediate interaction with different Rabs, and different sorting motifs can mediate interactions with the same Rab. For example, a dileucine motif in the C-terminus of  $\beta$ 2AR interacts with both Rab8 and Rab1 for anterograde trafficking to the plasma membrane (Dong *et al.*, 2010; Hammad *et al.*, 2012), and two basic residues in the C-terminal tail of the  $\beta$ 2AR and a five-amino acid MLERK motif in the cytoplasmic tail of the TRPV5 and TRPV6 cation channels both mediate interaction with GDP-Rab11 and recycling to the plasma membrane (van de Graaf *et al.*, 2006; Parent *et al.*, 2009). Alanine substitution of the PBM results in loss of p14 interaction with Rab11 (Figures 3 and 5), p14 accumulation in the Golgi complex (Figure 2), and reduced plasma membrane transport

(Parmar *et al.*, 2014b). It is conceivable that specific basic residues in the p14 PBM could promote direct interaction with GTP-Rab11, similar to the role of the two basic residues in the  $\beta$ 2AR C-terminal tail that mediate direct interaction with GDP-bound Rab11 (Parent *et al.*, 2009).

Mutational analysis, however, argues against the p14 PBM functioning as a specific protein-protein interaction motif. Every basic residue in the PBM can be substituted by alanine, individually or in various combinations, with little to no effect on p14 trafficking to the plasma membrane (Parmar *et al.*, 2014b). The only requirement for the PBM to promote p14 exit from the Golgi is a minimum of three positive charges (Parmar *et al.*, 2014b), indicating that it functions as a sequence-independent, electrostatic interaction motif. One possibility is the PBM may mediate interaction with anionic lipid head groups, such as those present in phosphoinositide (PI) lipids. Localized distribution of different PI species in distinct organelles and subdomains of a particular organelle is an important regulator of protein trafficking (Vicinanza *et al.*, 2008), including regulation of AP-1 localization to the TGN, which is promoted by AP-1 binding to phosphatidylinositol 4-phosphate (PI4P; Wang *et al.*, 2003). Accordingly, interaction of the p14 PBM with PI4P and activated Rab11 could colocalize this complex with AP-1 at the TGN for assembly into AP-1-coated vesicles (Figure 9).

How activated Rab11 mediates p14 incorporation into AP-1-coated vesicles is unknown, but several lines of evidence suggest the likelihood that this may involve Rab regulation of small GTPase cascades that promote coat protein assembly. For example, in yeast, the Golgi Arf-GEF Sec 7, an effector of Ypt31/32 and Ypt1 (homologues of Rab 11 and Rab1, respectively), activates the Arf1 small GTPase to recruit adaptor complexes at the TGN (McDonold and Fromme, 2014). Furthermore, in addition to AP-1 interactions with PI4P, binding sites for Arf-family GTPases in the  $\gamma$  and  $\beta$ 1 subunits of AP-1 promote AP-1 localization to the TGN and recycling endosomes (Ren *et al.*, 2013; Park and Guo, 2014). Activated GTP-Rab11 has also been shown to activate the GEF function of

Rab18, thereby activating Rab8 to regulate downstream vesicular trafficking (Knodler *et al.*, 2010). It therefore seems likely that future studies may identify similar small GTPase cascades that are regulated by p14 interactions with Rab11 at the TGN to generate AP-1-coated vesicles for exocytic trafficking of p14 from the Golgi complex.

## MATERIALS AND METHODS

### Cells and antibodies

HeLa cells were maintained in DMEM (Life Technologies, Carlsbad, CA) supplemented with 10% fetal bovine serum (FBS; Life Technologies). HEK cells were maintained in DMEM supplemented with 10% FBS and 25 mM 4-(2-hydroxyethyl)-1-piperazineethanesulfonic acid (Life Technologies). Rabbit polyclonal anti-p14 and anti-p14 ectodomain (anti-p14ecto) antibodies were previously described (Corcoran and Duncan, 2004; Top *et al.*, 2005). Antibodies against actin (Sigma-Aldrich, St. Louis, MO), Rab11A (BD Biosciences, Franklin Lakes, NJ), AP-1 $\gamma$  (Sigma-Aldrich), AP-3 $\delta$  (Developmental Studies Hybridoma Bank, Iowa City, IA), AP-4 $\epsilon$  (Abcam, Cambridge, MA), PI4KIII $\beta$  (BD Biosciences), TGN46 (AbD Serotech, Oxford, UK), horseradish peroxidase (HRP)-conjugated goat anti-rabbit (Jackson ImmunoResearch, West Grove, PA), HRP-conjugated goat anti-mouse (Santa Cruz Biotechnology, Dallas, TX), Alexa 488-conjugated goat anti-mouse and donkey anti-sheep, Alexa 555-conjugated donkey anti-rabbit, and Alexa-647-conjugated goat anti-rabbit and chicken anti-mouse (Life Technologies) were obtained from the indicated suppliers.

### Plasmids and transfection

The p14-G2A nonfusogenic p14 point substitution construct in pcDNA3 (referred to simply as p14) and the polybasic mutant of this construct containing alanine substitutions of the six basic residues (referred to as p14PA) were described previously (Corcoran and Duncan, 2004; Parmar *et al.*, 2014b). Rab11A cDNA was cloned into pcDNA3 using *Bam*HI and *Eco*RI restriction sites. Dominant-negative (Rab11-S25N) and constitutively active (Rab11-Q70L) forms of Rab11 were generated by site-directed mutagenesis (Stratagene, La Jolla, CA). Rab5 wild-type and dominant-negative (Rab5-S34N) constructs in pcDNA3 vector were kindly provided by Denis Dupré (Dalhousie University, Halifax, Canada). Plasmid pIRES-AP1G1 expressing the FKBP-tagged AP-1 $\gamma$  subunit (Robinson *et al.*, 2010) was obtained from Addgene (Cambridge, MA). The p14 and p14PA proteins were C-terminally tagged with EGFP or mCherry, and Rab11A and Rab11-S25N were similarly N-terminally tagged using overhanging PCR primers to subclone these constructs into pcDNA3. Plasmids were transfected into subconfluent monolayers of HeLa or HEK cells using Lipofectamine LTX (Life Technologies) or polyethyleneimine (Polysciences, Warrington, PA), respectively, according to manufacturer's instructions.

### Western blotting

Transfected HeLa or HEK cells were harvested by adding 2 $\times$  Laemmli's sample buffer directly onto the cells, scraped, syringed or sonicated, and boiled before separation by SDS-PAGE (7.5% or 15% acrylamide). Proteins were transferred onto polyvinylidene fluoride membranes, membranes were blocked with 5% milk in TBST (50 mM Tris-HCl, 150 mM NaCl, 0.1% Tween 20) for 1 h at room temperature, and probed with anti-actin (1:5000), anti-p14 (1:20,000), anti-Rab11A (1:5000), anti-AP1 $\gamma$  (1:5000), anti-AP3 $\delta$  (1:1000), or anti-AP4 $\epsilon$  (1:1000) primary antibodies at 4°C overnight. Blots were washed extensively with TBST and treated with HRP-conjugated goat anti-rabbit (1:10,000) or goat anti-mouse (1:5000) secondary antibodies for 1 h at room temperature. Membranes were developed using ECL+ reagent (Pierce, Waltham, MA) and imaged using a Typhoon 9410 variable-mode imager (GE Healthcare, Little Chalfont, UK). Blots

from two or more independent experiments were quantified using ImageJ (National Institutes of Health, Bethesda, MD).

### Coimmunoprecipitation

HEK cells transfected with p14, p14PA or empty vector were harvested at 24 hpt using a Rho-activation assay protocol (Cytoskeleton, Denver, CO). Briefly, cells were washed quickly with ice-cold phosphate-buffered saline (PBS), lysed on ice with ice-cold lysis buffer (50 mM Tris-HCl, pH 8.0, 0.5 M NaCl, 10 mM MgCl<sub>2</sub>, 2% IGEPAL), collected in microcentrifuge tubes by scrapping, syringed, and centrifuged at 14,000  $\times$  g for 5 min in a table-top centrifuge. Supernatants were snap-frozen in liquid nitrogen and stored at -80°C until use or incubated immediately with Dynabeads (Life Technologies) bound to Rab11 antibody or IgG isotype control for 1 h at 4°C. Samples were washed three times with lysis buffer and eluted by boiling the beads in 2 $\times$  Laemmli sample buffer. Eluted samples were separated by SDS-PAGE and analyzed by Western blotting with anti-p14 antibody. Aliquots of the cell lysates were removed before addition of Dynabeads and analyzed by Western blotting with anti-p14, anti-Rab11, and anti-actin antibodies to ensure protein expression, and equivalent protein loads were used for immunoprecipitation. For Rab11 activation, a GTP $\gamma$ S loading protocol was followed (Cytoskeleton). Cell lysates were treated with 10 mM EDTA and GTP $\gamma$ S (100  $\mu$ M) or GDP (1 mM) and incubated at 30°C for 30 min, then treated with 60 mM MgCl<sub>2</sub> before incubation of cell lysates with Rab11 antibody.

### RNA interference

Specific siRNAs targeting Rab11A and/or Rab11B (Wilson *et al.*, 2005; Sigma-Aldrich) or pools of siRNAs targeting AP-1 $\gamma$ , AP-3 $\delta$ , or AP-4 $\epsilon$  (SMARTpool; Dharmacon) were transfected for 48 h into HeLa cells using DharmaFECT1 transfection reagent (Dharmacon, Lafayette, CO) according to manufacturer's instructions. Cells were then analyzed by Western blotting to determine the efficiency of knockdown or were retransfected with p14, p14PA, or p14 and AP-1 and analyzed 24 h later by flow cytometry for p14 cell surface expression or by immunofluorescence microscopy to examine intracellular p14 localization.

### Cell surface immunofluorescence

HeLa cells were cotransfected with p14-G2A and Rab11, Rab11S25N, Rab11Q70L, Rab5, or Rab5S34N for 24 h or transfected with Rab11, AP1 $\gamma$ , AP3 $\delta$ , or AP4 $\epsilon$  siRNA for 48 h and retransfected with p14 or p14 and AP-1 for 24 h. Live transfected cells were treated with blocking buffer (1% BSA, 5% normal goat serum, 0.02% Na<sub>3</sub>N in Hanks' balanced salt solution) at 4°C for 30 min. Cells were then labeled with anti-p14ecto antibody (1:1000) for 1 h at 4°C, washed 3 $\times$  with blocking buffer, and incubated with Alexa 647-conjugated goat anti-rabbit antibody (1:2000) for 1 h at 4°C. Cells were washed 3 $\times$  with blocking buffer and then with ice-cold PBS, resuspended in PBS plus 10 mM EDTA, and fixed with 3.7% formaldehyde. We analyzed 10,000 cells by flow cytometry (FACSCalibur; BD Biosciences) using FCS Express software (De Novo). Cells transfected with empty vector were used as a negative control for immunostaining. Cell surface fluorescence was quantified by determining mean fluorescence intensity, and background fluorescence from empty vector-transfected cells was subtracted before calculating percentage surface fluorescence.

### Transferrin binding assay

At 24 hpt, HeLa cells transfected with Rab5 or Rab5S34N were incubated at 4°C for 10 min before addition of Alexa 647-conjugated transferrin (20  $\mu$ g/ml; Molecular Probes, Eugene, OR) for 20 min at

4°C. Cells were then washed with PBS, resuspended in PBS plus 10 mM EDTA, fixed with 3.7% formaldehyde, and analyzed by flow cytometry as described for cell surface immunofluorescence.

### Intracellular immunofluorescence microscopy

HeLa cells grown on glass coverslips were transfected with p14 or p14PA, fixed at 24 hpt with 3.7% formaldehyde for 20 min at room temperature, and permeabilized with 0.1% Triton X-100 for 20 min at room temperature. Cells were washed 3× with PBS and blocked for 30 min at room temperature with 1% BSA in PBS and colabeled in blocking buffer with anti-p14 (1:200), anti-Rab11 (1:100), anti-PI4KIIIβ (1:1000), anti-TGN46 (1:1000), or anti-AP1γ (1:1000) primary antibodies as required for 1 h at room temperature. Cells were then washed 3× with PBS and incubated with appropriate Alexa-conjugated secondary antibodies (1:1000) for 1 h at room temperature. Cells were mounted on glass slides after 3× washes with PBS using ProLong Gold antifade reagent (Life Technologies). Cells were imaged using a Zeiss LSM 510 META confocal microscope with 40× or 63× objective lens, and images were acquired in the focal plane of the Golgi complex. Colocalization was quantified from 10–20 cells from each of two independent experiments by calculating Pearson's *r* using the Coloc-2 plug-in of Fiji for ImageJ (Schindelin *et al.*, 2012).

### FRET assay

HeLa cells grown on coverslips were cotransfected with C-terminally EGFP-tagged p14 and N-terminally mCherry-tagged Rab11 constructs. Cells were fixed at 24 hpt with 3.7% formaldehyde, washed 3× with PBS, and mounted directly on glass slides using ProLong Gold antifade reagent. Images were taken with a Zeiss LSM 510 META confocal microscope using a 100× oil-immersion, 1.4 numerical aperture Plan Apochromat objective lens. For microscope setup and controls, cells were transfected with free EGFP, free mCherry, free EGFP and mCherry together, and EGFP linked to mCherry. For a bimolecular FRET positive control, p14-EGFP and p14-mCherry were cotransfected as a known homomultimeric protein. Cells were also cotransfected with p14-EGFP/mCherry-Rab11S25N and p14PA-EGFP/mCherry-Rab11 for FRET analysis. Cells cotransfected with free EGFP/mCherry-Rab11 and p14-EGFP/free mCherry were used as a FRET negative control. The donor and acceptor SBT values were visually minimized using free EGFP- and free mCherry-transfected cells, respectively. FRET intensity signals were then determined, and a series of three images was taken for each sample: 1) Donor image with donor excitation and donor emission, 2) acceptor image with acceptor excitation and acceptor emission, and 3) FRET image with donor excitation and acceptor emission. Background subtraction and Gaussian blur for donor, acceptor, and FRET channels were performed on each image, and NFRET intensities were obtained by pixel-by-pixel FRET analysis of images using the PixFRET ImageJ plug-in, which adjusts for differences in protein expression levels between cells (Feige *et al.*, 2005). NFRET images were converted into 8-bit images for histogram analysis and to obtain mean NFRET values for individual cells. Mean NFRET values for 10 cells each from each of two independent experiments were obtained for statistical analysis.

### Statistics

Statistical analysis and sample comparison were performed using Prism software (GraphPad, San Diego, CA). SEM values were calculated for averaging sample values between experiments. Groups of two samples were analyzed with a paired two-tailed *t* test, and groups of more than two samples were analyzed using analysis of variance (ANOVA) with a Tukey posttest.

## ACKNOWLEDGMENTS

We thank Neale Ridgway, Craig McCormick, and Denis Dupré (Dalhousie University, Halifax, Canada) for providing antibodies and reagents. This work was funded by a grant to R.D. from the Natural Sciences and Engineering Research Council of Canada.

## REFERENCES

- Aloisi AL, Bucci C (2013). Rab GTPases-cargo direct interactions: fine modulators of intracellular trafficking. *Histol Histopathol* 28, 839–849.
- Ang AL, Taguchi T, Francis S, Folsch H, Murrells LJ, Pypaert M, Warren G, Mellman I (2004). Recycling endosomes can serve as intermediates during transport from the Golgi to the plasma membrane of MDCK cells. *J Cell Biol* 167, 531–543.
- Bankaitis VA, Garcia-Mata R, Mousley CJ (2012). Golgi membrane dynamics and lipid metabolism. *Curr Biol* 22, R414–424.
- Barr FA (2013). Review series: Rab GTPases and membrane identity: causal or inconsequential? *J Cell Biol* 202, 191–199.
- Boutillier J, Duncan R (2011). The reovirus fusion-associated small transmembrane (FAST) proteins: virus-encoded cellular fusogens. *Curr Top Membr* 68, 107–140.
- Brewer CB, Roth MG (1991). A single amino acid change in the cytoplasmic domain alters the polarized delivery of influenza virus hemagglutinin. *J Cell Biol* 114, 413–421.
- Cancino J, Torrealba C, Soza A, Yuseff MI, Gravotta D, Henklein P, Rodriguez-Boulan E, Gonzalez A (2007). Antibody to AP1B adaptor blocks biosynthetic and recycling routes of basolateral proteins at recycling endosomes. *Mol Biol Cell* 18, 4872–4884.
- Caswell PT, Spence HJ, Parsons M, White DP, Clark K, Cheng KW, Mills GB, Humphries MJ, Messent AJ, Anderson KI, *et al.* (2007). Rab25 associates with alpha5beta1 integrin to promote invasive migration in 3D microenvironments. *Dev Cell* 13, 496–510.
- Chen W, Feng Y, Chen D, Wandinger-Ness A (1998). Rab11 is required for trans-golgi network-to-plasma membrane transport and a preferential target for GDP dissociation inhibitor. *Mol Biol Cell* 9, 3241–3257.
- Cheng SB, Filardo EJ (2012). Trans-Golgi network (TGN) as a regulatory node for beta1-adrenergic receptor (beta1AR) down-modulation and recycling. *J Biol Chem* 287, 14178–14191.
- Cheng SB, Quinn JA, Graeber CT, Filardo EJ (2011). Down-modulation of the G-protein-coupled estrogen receptor, GPER, from the cell surface occurs via a trans-Golgi-proteasome pathway. *J Biol Chem* 286, 22441–22455.
- Ciechomska M, Key T, Duncan R (2014). Efficient reovirus- and measles virus-mediated pore expansion during syncytium formation is dependent on annexin A1 and intracellular calcium. *J Virol* 88, 6137–6147.
- Corcoran JA, Clancy EK, Duncan R (2011a). Homomultimerization of the reovirus p14 fusion-associated small transmembrane protein during transit through the ER-Golgi complex secretory pathway. *J Gen Virol* 92, 162–166.
- Corcoran JA, Clancy EK, Duncan R (2011b). Homomultimerization of the reovirus p14 fusion-associated small transmembrane protein during transit through the ER-Golgi complex secretory pathway. *J Gen Virol* 92, 162–166.
- Corcoran JA, Duncan R (2004). Reptilian reovirus utilizes a small type III protein with an external myristylated amino terminus to mediate cell-cell fusion. *J Virol* 78, 4342–4351.
- Donaldson JG, Jackson CL (2011). ARF family G proteins and their regulators: roles in membrane transport, development and disease. *Nat Rev Mol Cell Biol* 12, 362–375.
- Dong C, Yang L, Zhang X, Gu H, Lam ML, Claycomb WC, Xia H, Wu G (2010). Rab8 interacts with distinct motifs in alpha2B- and beta2-adrenergic receptors and differentially modulates their transport. *J Biol Chem* 285, 20369–20380.
- Feige JN, Sage D, Wahli W, Desvergne B, Gelman L (2005). PixFRET, an ImageJ plug-in for FRET calculation that can accommodate variations in spectral bleed-throughs. *Microsc Res Tech* 68, 51–58.
- Folsch H, Mattila PE, Weisz OA (2009). Taking the scenic route: biosynthetic traffic to the plasma membrane in polarized epithelial cells. *Traffic* 10, 972–981.
- Futter CE, Connolly CN, Cutler DF, Hopkins CR (1995). Newly synthesized transferrin receptors can be detected in the endosome before they appear on the cell surface. *J Biol Chem* 270, 10999–11003.
- Giraud CG, Maccioni HJ (2003). Endoplasmic reticulum export of glycosyltransferases depends on interaction of a cytoplasmic dibasic motif with Sar1. *Mol Biol Cell* 14, 3753–3766.

- Goldenring JR, Shen KR, Vaughan HD, Modlin IM (1993). Identification of a small GTP-binding protein, Rab25, expressed in the gastrointestinal mucosa, kidney, and lung. *J Biol Chem* 268, 18419–18422.
- Guo X, Mattera R, Ren X, Chen Y, Retamal C, Gonzalez A, Bonifacino JS (2013). The adaptor protein-1 mu1B subunit expands the repertoire of basolateral sorting signal recognition in epithelial cells. *Dev Cell* 27, 353–366.
- Hamelin E, Theriault C, Laroche G, Parent JL (2005). The intracellular trafficking of the G protein-coupled receptor TPbeta depends on a direct interaction with Rab11. *J Biol Chem* 280, 36195–36205.
- Hammad MM, Kuang YQ, Morse A, Dupre DJ (2012). Rab1 interacts directly with the beta2-adrenergic receptor to regulate receptor anterograde trafficking. *Biol Chem* 393, 541–546.
- Hirst J, Irving C, Borner GH (2013). Adaptor protein complexes AP-4 and AP-5: new players in endosomal trafficking and progressive spastic paraplegia. *Traffic* 14, 153–164.
- Honing S, Sandoval IV, von Figura K (1998). A di-leucine-based motif in the cytoplasmic tail of LIMP-II and tyrosinase mediates selective binding of AP-3. *EMBO J* 17, 1304–1314.
- Hunziker W, Fumey C (1994). A di-leucine motif mediates endocytosis and basolateral sorting of macrophage IgG Fc receptors in MDCK cells. *EMBO J* 13, 2963–2969.
- Hunziker W, Harter C, Matter K, Mellman I (1991). Basolateral sorting in MDCK cells requires a distinct cytoplasmic domain determinant. *Cell* 66, 907–920.
- Hutagalung AH, Novick PJ (2011). Role of Rab GTPases in membrane traffic and cell physiology. *Physiol Rev* 91, 119–149.
- Jia R, Xu F, Qian J, Yao Y, Miao C, Zheng YM, Liu SL, Guo F, Geng Y (2014). Identification of an endocytic signal essential for the antiviral action of IFITM3. *Cell Microbiol* 16, 1080–1093.
- Kelly EE, Horgan CP, McCaffrey MW (2012). Rab11 proteins in health and disease. *Biochem Soc Trans* 40, 1360–1367.
- Key T, Duncan R (2014). A compact, multifunctional fusion module directs cholesterol-dependent homomultimerization and syncytiogenic efficiency of reovirus p10 FAST proteins. *PLoS Pathog* 10, e1004023.
- Kikuchi A, Yamashita T, Kawata M, Yamamoto K, Ikeda K, Tanimoto T, Takai Y (1988). Purification and characterization of a novel GTP-binding protein with a molecular weight of 24,000 from bovine brain membranes. *J Biol Chem* 263, 2897–2904.
- Knodler A, Feng S, Zhang J, Zhang X, Das A, Peranen J, Guo W (2010). Coordination of Rab8 and Rab11 in primary ciliogenesis. *Proc Natl Acad Sci USA* 107, 6346–6351.
- Lai F, Stubbs L, Artzt K (1994). Molecular analysis of mouse Rab11b: a new type of mammalian YPT/Rab protein. *Genomics* 22, 610–616.
- Lock JG, Stow JL (2005). Rab11 in recycling endosomes regulates the sorting and basolateral transport of E-cadherin. *Mol Biol Cell* 16, 1744–1755.
- Mardones GA, Burgos PV, Lin Y, Kloer DP, Magadan JG, Hurley JH, Bonifacino JS (2013). Structural basis for the recognition of tyrosine-based sorting signals by the mu3A subunit of the AP-3 adaptor complex. *J Biol Chem* 288, 9563–9571.
- McDonold CM, Fromme JC (2014). Four GTPases differentially regulate the Sec7 Arf-GEF to direct traffic at the trans-golgi network. *Dev Cell* 30, 759–767.
- McEwen DP, Schumacher SM, Li Q, Benson MD, Iniguez-Lluhi JA, Van Genderen KM, Martens JR (2007). Rab-GTPase-dependent endocytic recycling of Kv1.5 in atrial myocytes. *J Biol Chem* 282, 29612–29620.
- Mellman I, Nelson WJ (2008). Coordinated protein sorting, targeting and distribution in polarized cells. *Nat Rev Mol Cell Biol* 9, 833–845.
- Nishimura N, Plutner H, Hahn K, Balch WE (2002). The delta subunit of AP-3 is required for efficient transport of VSV-G from the trans-Golgi network to the cell surface. *Proc Natl Acad Sci USA* 99, 6755–6760.
- Ohno H (2006). Clathrin-associated adaptor protein complexes. *J Cell Sci* 119, 3719–3721.
- Ohno H, Stewart J, Fournier MC, Bosshart H, Rhee I, Miyatake S, Saito T, Gallusser A, Kirchhausen T, Bonifacino JS (1995). Interaction of tyrosine-based sorting signals with clathrin-associated proteins. *Science* 269, 1872–1875.
- Parent A, Hamelin E, Germain P, Parent JL (2009). Rab11 regulates the recycling of the beta2-adrenergic receptor through a direct interaction. *Biochem J* 418, 163–172.
- Park SY, Guo X (2014). Adaptor protein complexes and intracellular transport. *Biosci Rep* 34.
- Parmar HB, Barry C, Duncan R (2014a). Polybasic trafficking signal mediates golgi export, ER retention or ER export and retrieval based on membrane-proximity. *PLoS One* 9, e94194.
- Parmar HB, Barry C, Kai F, Duncan R (2014b). Golgi complex-plasma membrane trafficking directed by an autonomous, tribasic Golgi export signal. *Mol Biol Cell* 25, 866–878.
- Pellinen T, Arjonen A, Vuoriluoto K, Kallio K, Fransén JA, Ivaska J (2006). Small GTPase Rab21 regulates cell adhesion and controls endosomal traffic of beta1-integrins. *J Cell Biol* 173, 767–780.
- Pfeffer SR (2013). Rab GTPase regulation of membrane identity. *Curr Opin Cell Biol* 25, 414–419.
- Popova NV, Deyev IE, Petrenko AG (2013). Clathrin-mediated endocytosis and adaptor proteins. *Acta Naturae* 5, 62–73.
- Rajasekaran AK, Humphrey JS, Wagner M, Miessenbock G, Le Bivic A, Bonifacino JS, Rodriguez-Boulán E (1994). TGN38 recycles basolaterally in polarized Madin-Darby canine kidney cells. *Mol Biol Cell* 5, 1093–1103.
- Ren X, Farias GG, Canagarajah BJ, Bonifacino JS, Hurley JH (2013). Structural basis for recruitment and activation of the AP-1 clathrin adaptor complex by Arf1. *Cell* 152, 755–767.
- Robinson MS, Sahlender DA, Foster SD (2010). Rapid inactivation of proteins by rapamycin-induced rerouting to mitochondria. *Dev Cell* 18, 324–331.
- Rodriguez-Boulán E, Kreitzer G, Musch A (2005). Organization of vesicular trafficking in epithelia. *Nat Rev Mol Cell Biol* 6, 233–247.
- Rzomp KA, Scholtes LD, Briggs BJ, Whittaker GR, Scidmore MA (2003). Rab GTPases are recruited to chlamydial inclusions in both a species-dependent and species-independent manner. *Infect Immun* 71, 5855–5870.
- Sakurada K, Uchida K, Yamaguchi K, Aisaka K, Ito S, Ohmori T, Takeyama Y, Ueda T, Hori Y, Ohyanagi H, et al. (1991). Molecular cloning and characterization of a ras p21-like GTP-binding protein (24KG) from rat liver. *Biochem Biophys Res Commun* 177, 1224–1232.
- Santiago-Tirado FH, Bretscher A (2011). Membrane-trafficking sorting hubs: cooperation between PI4P and small GTPases at the trans-Golgi network. *Trends Cell Biol* 21, 515–525.
- Schindelin J, Arganda-Carreras I, Frise E, Kaynig V, Longair M, Pietzsch T, Preibisch S, Rueden C, Saalfeld S, Schmid B, et al. (2012). Fiji: an open-source platform for biological-image analysis. *Nat Methods* 9, 676–682.
- Somsel Rodman J, Wandering-Ness A (2000). Rab GTPases coordinate endocytosis. *J Cell Sci* 113, 183–192.
- Sekar RB, Periasamy A (2003). Fluorescence resonance energy transfer (FRET) microscopy imaging of live cell protein localizations. *J Cell Biol* 160, 629–633.
- Stenmark H (2009). Rab GTPases as coordinators of vesicle traffic. *Nat Rev Mol Cell Biol* 10, 513–525.
- Takahashi M, Ishiko T, Kamohara H, Hidaka H, Ikeda O, Ogawa M, Baba H (2007). Curcumin (1,7-bis(4-hydroxy-3-methoxyphenyl)-1,6-heptadiene-3,5-dione) blocks the chemotaxis of neutrophils by inhibiting signal transduction through IL-8 receptors. *Mediators Inflamm* 2007, 10767.
- Top D, de Antueno R, Salsman J, Corcoran J, Mader J, Hoskin D, Touhami A, Jericho MH, Duncan R (2005). Liposome reconstitution of a minimal protein-mediated membrane fusion machine. *EMBO J* 24, 2980–2988.
- van de Graaf SF, Chang Q, Mensenkamp AR, Hoenderop JG, Bindels RJ (2006). Direct interaction with Rab11a targets the epithelial Ca<sup>2+</sup> channels TRPV5 and TRPV6 to the plasma membrane. *Mol Cell Biol* 26, 303–312.
- Vicinanza M, D'Angelo G, Di Campli A, De Matteis MA (2008). Function and dysfunction of the PI system in membrane trafficking. *EMBO J* 27, 2457–2470.
- Wang YJ, Wang J, Sun HQ, Martínez M, Sun YX, Macia E, Kirchhausen T, Albanesi JP, Roth MG, Yin HL (2003). Phosphatidylinositol 4 phosphate regulates targeting of clathrin adaptor AP-1 complexes to the Golgi. *Cell* 114, 299–310.
- Welz T, Wellbourne-Wood J, Kerkhoff E (2014). Orchestration of cell surface proteins by Rab11. *Trends Cell Biol* 24, 407–415.
- Wikstrom K, Reid HM, Hill M, English KA, O'Keefe MB, Kimbembe CC, Kinsella BT (2008). Recycling of the human prostacyclin receptor is regulated through a direct interaction with Rab11a GTPase. *Cell Signal* 20, 2332–2346.
- Wilson C, Venditti R, Rega LR, Colanzi A, D'Angelo G, De Matteis MA (2011). The Golgi apparatus: an organelle with multiple complex functions. *Biochem J* 433, 1–9.
- Wilson GM, Fielding AB, Simon GC, Yu X, Andrews PD, Hames RS, Frey AM, Peden AA, Gould GW, Prekeris R (2005). The FIP3-Rab11 protein complex regulates recycling endosome targeting to the cleavage furrow during late cytokinesis. *Mol Biol Cell* 16, 849–860.
- Zimmermann R, Eyrich S, Ahmad M, Helms V (2011). Protein translocation across the ER membrane. *Biochim Biophys Acta* 1808, 912–924.